coatings

MDPI

Article

Study of the Durability and Aesthetical Properties of Powder Coatings Admixed with Pearlescent Pigments

Stefano Rossi *, Francesca Russo and Lotfi Bouchakour Rahmani

Department of Industrial Engineering, University of Trento, Via Sommarive 9, 38123 Trento, Italy; francesca.russo-2@unitn.it (F.R.); cjls@libero.it (L.B.R.)

* Correspondence: stefano.rossi@unitn.it; Tel.: +39-0461-282442

Received: 30 January 2020; Accepted: 28 February 2020; Published: 3 March 2020

Abstract: Powder coatings are commonly used to protect metallic substrates because of their good protection properties together with their aesthetical ones. In this work, the aesthetic and functional properties of powder coatings admixed with pearlescent pigments were investigated. The main aim of this work is represented by the evaluation of the coating properties and their change assessment after accelerated ageing treatments, such as UV and salt spray exposure. Changes in gloss, color and roughness were recorded before, during, and after UVA and UVB exposure. All the samples showed good resistance to UVA irradiation, whereas UVB light caused a huge variation in surface properties. Further insights on the degradation of the polymeric matrix were gained by exploiting FT-IR analyses, which could be correlated to the change of color. The protection properties of the coating were assessed by exploiting an acetic salt spray test. All the samples showed good resistance to aggressive environments, and no pigment effect on the degradation of the coatings could be detected.

Keywords: pearlescent pigments; powder coatings; durability; ageing treatments

1. Introduction

Nowadays, the main challenge of materials engineering is the modification of the surface characteristics of a substrate in order to improve its functional properties for high duty technological applications. In the last decades, the development of a coating has increasingly focused on finding materials with surprising functional properties that also had good perceptive and aesthetical characteristics [1]. In this context, organic coatings are employed to guarantee the good protection of metal products, combining a high sustainability of the industrial deposition process [1] with the possibility of obtaining a high variety of surface aesthetic effects. Thus, the evaluation of the aesthetical properties is a key factor to take under consideration when studying the coating performances [2]. Among all the different types of protective layers, powder coatings are arousing increasing interest in the building, automotive, and cosmetic industry, mainly due to the low environmental and economic impact they entail and for the wide range of pigments available on the market [3]. Pigments consist of insoluble powders dispersed in the coating matrix, and they can be either organic or inorganic, though the latest type is the most used [4]. To understand the industrial importance of pigment production, it is sufficient to report that in 2005 the world production of inorganic pigments was approximately equal to 6 million tons, of which at least half was for the production of high-performance pigments [5]. The industrial research on pigments has recently focused on three main roads: the economization of already existing pigments, the discovery and development of inorganic pigments with better performance features, and the replacement of some toxic and non-ecological chemical substances in order to be in compliance with new national and international regulations [6,7].

Pigments can be classified in different ways, according, for example, to the way they interact with light; among them, this work will focus on the special effects pigments, and in particular on pearlescent

pigments [8]. Pearlescent pigments give the coating additional color effects, such as an angular color dependence, which is mainly due to the interference of light on thin layers, flakes, or platelets [9]. The industrial production of pearlescent pigments started during the 1920s using mercury and arsenic salts. In 1963, the discovery of new TiO_2-coated mica pigments was reported, and only in the 1990s were effect pigments, based on aluminum platelets and coated with ferric oxide, introduced into the market [10].

Effect pigments can be basically divided into two types: substrate-free pigments and layered pigments. The first show a brittle behavior, and their use is limited by their chemical composition, whereas the latter are produced by coating thin laminar platelets of mica or alumina with high refractive optical layers, such as titanium dioxide, iron oxide, or a combination of both [11]. Most pearlescent pigments have at least three layers of two different materials with different refractive indexes. The pearlescent effect is produced by the specular reflection of light from the many surfaces of the platelets at various depths within the coating film. Light striking the platelet is partially reflected and partially transmitted through the platelet; the pearlescent effect is produced by the dependence of the reflection on the viewing angle [12]. Alumina-based pigments have a strong pearlescent effect with respect to mica-based pigments because they are easily produced, with a very narrow thickness distribution and very smooth surfaces [11]. In the last decade, this type of pigments has found a broad application range, both for decorative and functional purposes [13,14], also thanks to the ease of incorporation in the coating matrix [11]. Alumina-based pigments exhibit the well-known advantages of mica pigments together with the possibility of realizing unique optical effects thanks to their controlled thickness and chemical purity [11].

This study is focused on the characterization of powder coatings with the addition of innovative alumina-based pearlescent pigments. This type of pigments has got enhanced optical properties and shows great pearlescent behavior with respect to mica-based pigments, but no studies about their effect on the durability of the coatings can be found in the literature. The main aim of this work is represented by the evaluation of coatings' aesthetical and functional properties and their change assessment as a consequence of accelerated ageing treatments, such as UV and salt spray exposure.

2. Materials and Methods

The superdurable powder coatings Interpon D2525, based on isophthalic acid (IPA) polyester resin and TGIC-free, were supplied by Akzo Nobel Coatings S.p.A. (Como, Italy) and were applied on $150 \times 60 \times 0.75$ mm^3 5005 aluminum alloy panels. Regarding the coating formulation, five different pigment types, supplied by Merck S.p.A (Darmstadt, Germany), were added to the polymeric matrix, thus obtaining the five sample series reported in Table 1. In the premixing phase, a special treatment, consisting in raising the temperature by a few degrees above the matrix glass transition temperature (T_g), was exploited in order to obtain a very homogeneous powder, allowing the pigments to be uniformly dispersed. Therefore, the layers were applied by an electrostatic spray deposition method and cured at 200 °C for 15 min.

Table 1. Nomenclature of the samples with the component formulation.

Coating Name	Pigment Type	Pigment wt.%	Powder Coating wt.%
GB-SW	Xirallic T60-23 SW Galaxy Blue	4.00	96.00
GB-WNT	Xirallic T60-23 WNT Galaxy Blue	4.00	96.00
LG	Xirallic NXT M260-30 SW Leonis Gold	4.00	96.00
PS	Xirallic NXT M60-69 WNT Panthera Silver	4.00	96.00
TB	Xirallic NXT M260-23 Tigris Blue	4.00	96.00

The pigments color and morphology were studied by optical and electron microscopy, by means of Nikon SMZ25 stereomicroscope (Nikon Instruments, Amstelveen, Netherlands) and JEOL IT300 Scanning Electron Microscope (SEM, Jeol Ltd., Akishima, Tokyo, Japan) microscope, respectively. Moreover, SEM observations were employed in the coatings and pigments thickness assessment. The chemical composition of the pigments was analyzed by Energy Dispersive X-Ray Spectrometry (EDS), carried out using a Bruker "Quantax Micro-XRF" analyzer (Billerica, MA, USA). The influence of the environment on the aesthetical properties of the coatings was assessed by exposing the five sample series to UV radiation (UVA and UVB radiation for times up to 1000 h). UV radiation is responsible for the degradation processes of organic coatings, since the associated energy is sufficient to break the C–H and C–C bonds of the polymer. UVA and UVB radiations are distinguished by the wavelength range, which ranges from 400 to 320 nm for UVA light and from 320 to 280 nm for UVB light. UV light accelerated tests were carried out using a UVA-340 lamp and a UVB-313EL lamp with emission peaks at 340 and 313 nm, respectively, as described by the ASTM G154 (2016) standard [15], in order to check how different radiation types affected the degradation of the coating. The changes of aesthetical properties were also evaluated by exploiting color measurements, using the spectrophotometer CM-2600d Konica Minolta, with a D65/10° illuminant/observer, and also by exploiting gloss and roughness measurements, according to the ASTM D523-14 (2018) [16] standard and ISO 4288 (1996) standard [17], respectively. The gloss measurements were collected using an Erichsen NL3A glossmeter (Westlake, OH, USA), acquiring the values for the residual gloss at 60°. Every reported value represents the average of six measurements. The roughness data were acquired by means of the MAHR Marsurf PS1 roughness tester (Esslingen, Germany). A sampling length (l_r) of 0.8 mm and an evaluation length (l_n) of 5.6 mm was used; the reported value is the average of five measurements. In order to check the deterioration of the coating organic matrix, IR spectra were collected between 4000 and 600 cm^{-1} before and after UVA and UVB exposure, using the spectrophotometer Varian 4100 FT-IR with a resolution of 4 cm^{-1} (Palo Alto, CA, USA). Regarding the protection properties of the coating, accelerated corrosion testing was exploited in an acetic acid salt spray chamber on as-made samples and also on samples with the presence of an artificial notch. The samples were exposed for times up to 1000 h to a salt spray solution produced by a 5 wt.% NaCl solution at 35 °C and 100% RH, according to the ASTM B117-19 (2019) standard [18], with the addition of acetic acid in order to vary the pH between 3.1 and 3.3, thus avoiding the passivation of Al substrate at neutral pH, as described by the ASTM G85-19 (2019) standard [19]. As a first thing, the salt spray test was involved in the study of the blister evolution and detachment grade of the coating, by making a cross-cut incision of 1 mm width down to the metal, as specified by the UNI EN ISO 4628-8 (2013) [20]. In addition to that, Electrochemical Impedance Spectroscopy (EIS) measurements were carried out on as-made samples after 0, 400, 750, and 1000 h of exposition in a salt spray chamber, in order to evaluate the protection properties of the coatings. The measurements have been exploited in 5 wt.% NaCl solution and using a three-electrode configuration: a platinum electrode was used as a counter electrode, and an Ag/AgCl electrode was used as a reference. The tested area was 4.9 cm^2. A signal amplitude of 30 mV in the frequency range from 10^6 to 10^{-2} Hz was set up.

3. Results

3.1. Morphology and Chemical Characterization

Figure 1 shows the morphology of the pigment flakes. The pigments are free-flowing powders, and their average diameter dimension is included between 10 and 30 μm. From a detailed SEM analysis at high magnifications, it is also possible to assess the pigments' thickness, which resulted as being about 550, 590, 660, 250, and 460 nm for the GB-SW, GB-WNT, LG, PS, and TB pigments, respectively. The difference in thickness among the pigments, which is lower than 1 μm in all cases, can also be noticed from their different transparency to electrons, in particular regarding the PS and TB pigments (Figure 1).

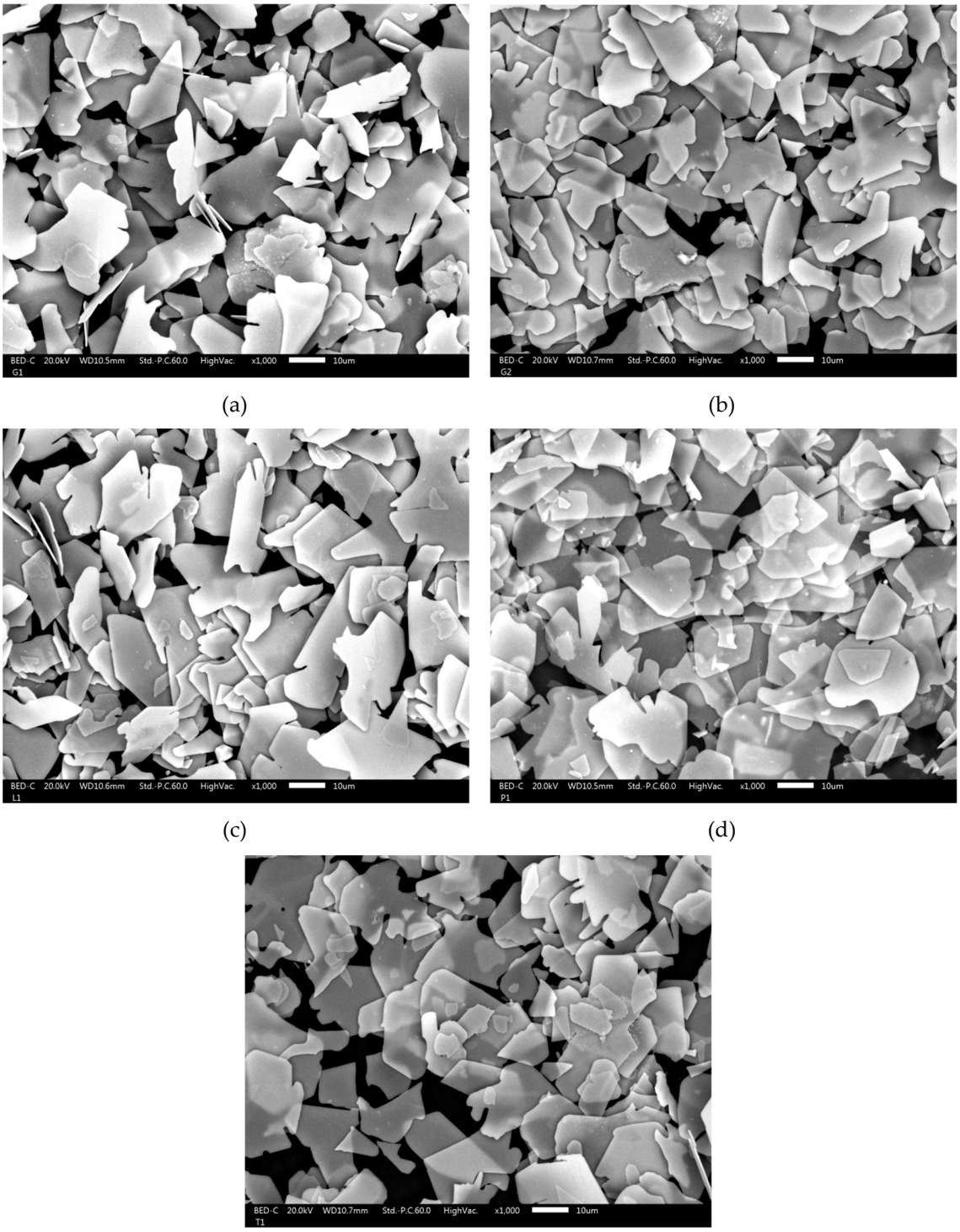

Figure 1. SEM images of pigment flakes: (**a**) GB-SW; (**b**) GB-WNT; (**c**) LG; (**d**) PS; and (**e**) TB.

The chemical composition of the pigments was investigated through a semiquantitative EDS analysis, whose results in atomic percentages are reported in Table 2. The results are extrapolated by a fitting operated by the Esprit Bruker software (2.0).

Table 2. EDS analysis of the studied pigments.

Pigment	O %	Si %	Al %	Ti %	Sn %	Zr %	Fe%	Cu %
Xirallic T60-23 SW Galaxy Blue	51.0	1.4	28.1	18.1	1.4	–	–	–
Xirallic T60-23 WNT Galaxy Blue	48.4	1.3	31.4	18.1	0.3	0.3	0.1	0.1
Xirallic NXT M260-30 SW Leonis Gold	40.6	0.8	29.1	10.7	1.0	–	17.8	–
Xirallic NXT M60-69 WNT Phantera Silver	49.2	0.5	41.5	5.9	0.2	0.6	2.1	–
Xirallic NXT M260-23 Tigris Blue	52.1	1.4	28.4	17.8	0.3	–	–	–

Comparing the five different pigment types, it is possible to detect for all of them a high presence of aluminum and titanium: aluminum, present as α-Al_2O_3, is the main component of the pigment substrate, whereas titanium, deposited as TiO_2 on the substrate, is used as an optical layer, together with other oxides, present at lower concentrations [11]. All the samples show the presence of silicon and tin, used to promote the nucleation of the rutile phase of TiO_2. The presence of the rutile phase is to be preferred to the anatase one, because the latter has a lower photocatalytic activity. Several studies have reported on the investigation of the effect of different elements on the rutile-anatase phase transformation in pearlescent pigments: the presence of tin oxide, in the crystalline form of casserite, should promote the epitaxial growth of the rutile phase, thanks to the perfect match between their cell parameters [21,22]. The Leonis Gold pigment contains a very high amount of Fe, also present as an oxide, to which the intense yellow color of the pigment and the high light interference effect are attributable. Only the Galaxy Blue WNT and Panthera Silver pigments show the presence of zirconium oxide, which is a high-refractive material and which is in widespread use for the synthesis of pearlescent pigments [23].

The SEM micrographs in Figure 2 show the as-deposited sample cross sections. All the sample cross-sections highlight a good and homogeneous dispersion of the pigments inside the polymeric matrix. The random orientation of the pigments, as shown in Figure 2, has a positive effect in harvesting the coating pearlescent effect. The thickness of the samples can be also evaluated from the SEM micrographs in Figure 2, and its value is between 75 and 150 µm. The high thickness dispersion of the coating is typical of powder coatings obtained by spray deposition and does not affect the properties under investigation.

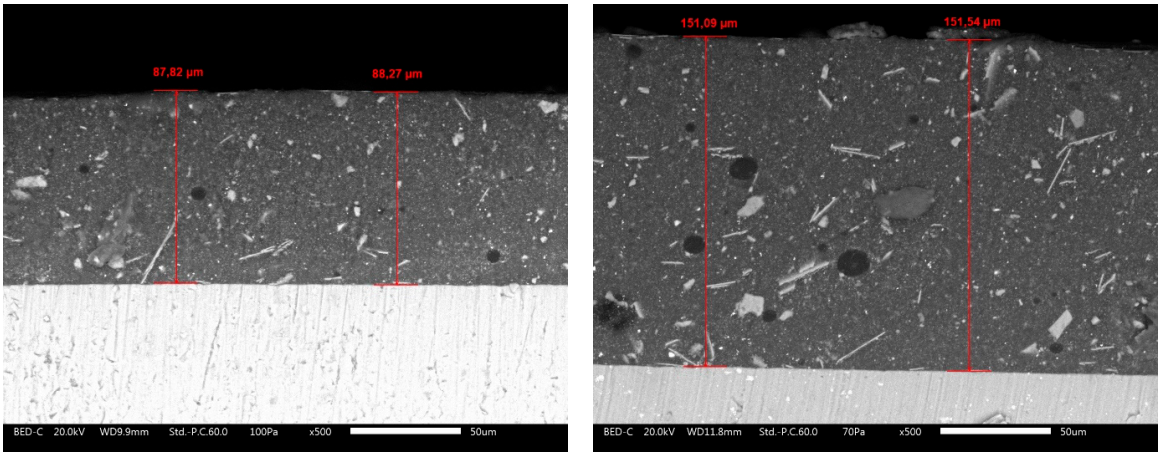

(a) (b)

Figure 2. *Cont.*

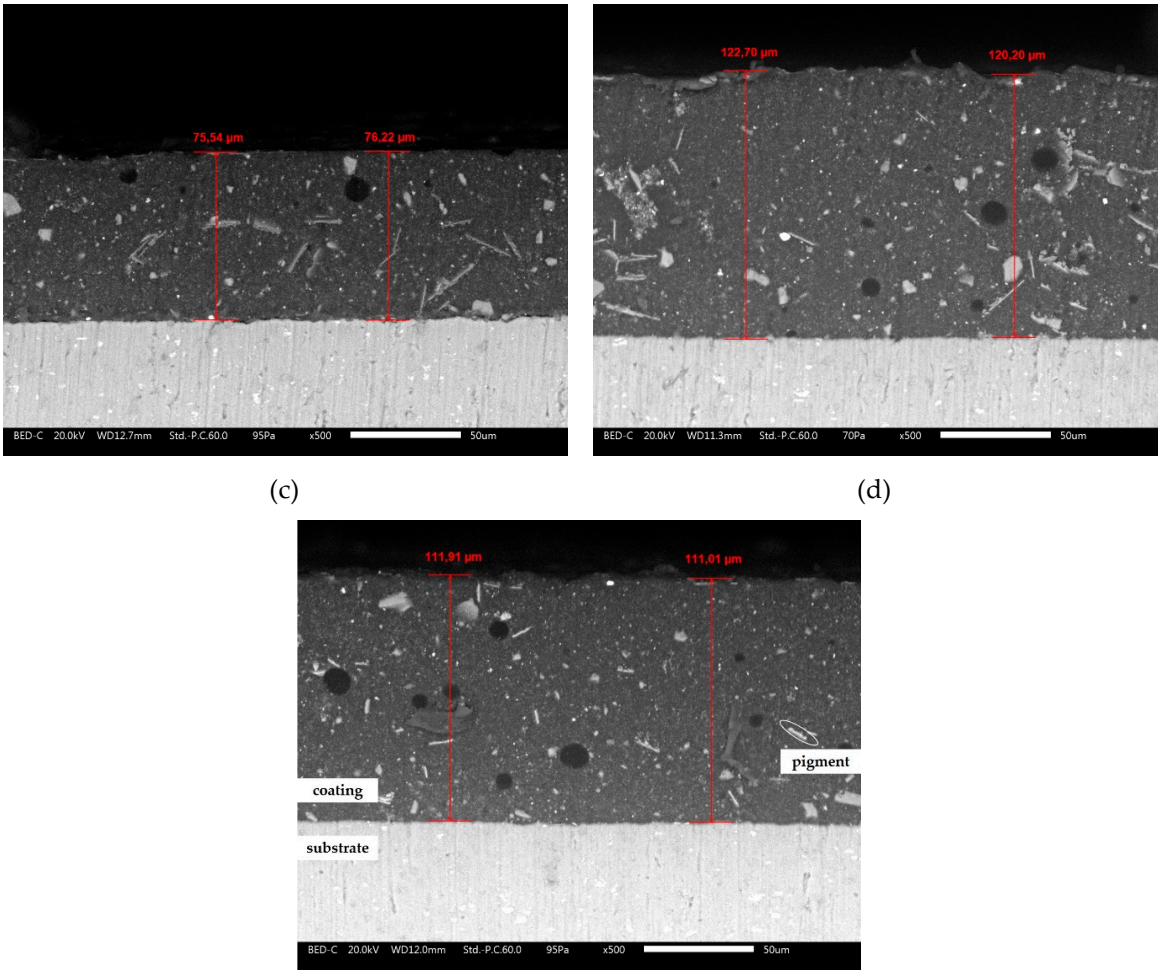

Figure 2. Scanning electron microscope cross sections of the sample: (**a**) GB-SW; (**b**) GB-WNT; (**c**) LG; (**d**) PS; and (**e**) TB. In (**e**), a description of the components of the sample is made.

3.2. Gloss and Roughness Evaluation after UV Exposure

The changes of the coating aesthetical properties were assessed after 1000 h UV exposure. Regarding the roughness change, the mean roughness parameter, R_a, was chosen in order to give the average information about the sample surface.

Table 3 shows the roughness variation for all the samples before and after UVA and UVB exposure. All the samples underwent an increase in roughness of about 0.1–0.2 µm after 1000 h of irradiation with UVB light, whereas a different behaviour after 1000 h UVA irradiation was verifiable. All the samples showed a decreased superficial roughness after UVA irradiation, apart from the LG sample, which showed a small increase. Considering the error bars, it is possible to state that the roughness values after UVA exposure could be comparable to the values of the pristine samples, and thus no significant changes could be seen after 1000 h of UVA exposure.

Table 3. Sample roughness before and after 1000 h irradiation with UVA and UVB light.

Coating Name	R_a As-Made (µm)	R_a 1000 h UVA (µm)	R_a 1000 h UVB (µm)
GB-SW	0.66 ± 0.08	0.65 ± 0.05	0.77 ± 0.33
GB-WNT	0.86 ± 0.24	0.79 ± 0.12	0.97 ± 0.10
LG	0.65 ± 0.04	0.69 ± 0.08	0.87 ± 0.08
PS	0.74 ± 0.14	0.69 ± 0.08	0.82 ± 0.12
TB	0.66 ± 0.11	0.59 ± 0.08	0.75 ± 0.11

The surface roughness influences the gloss of a surface: on a smooth mirror-like surface, parallel beams of light are reflected in the same certain direction, whereas on an irregular surface, beams of light are diffusely scattered, and the surface appears to be matt. Determining the gloss change is then important to have further insights on the modification of the sample surface properties. After 1000 h of UVA irradiation, the maximum gloss change was about 5%, and it was almost similar for all the samples. It did not follow a linear decreasing trend, but it remained stable over time. Gloss and roughness are closely interrelated, thus the small changes in roughness are connected and in accordance with the little changes in gloss of the samples. In contrast, with respect to what happened to the samples after irradiation with UVA light, it was possible to see a clear decreasing trend of gloss with the increase of the UVB light exposure time, as shown in Figure 3. All the samples showed the same behaviour, which is probably connected to the degradation of the polymeric matrix.

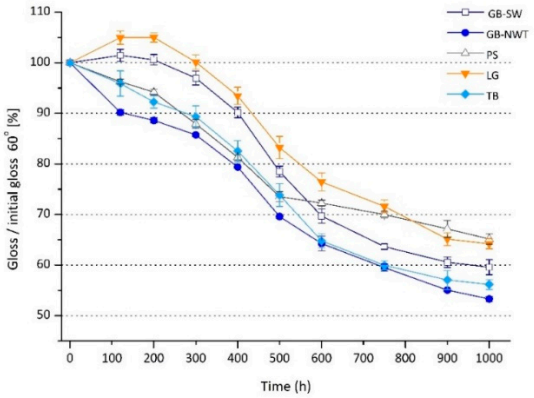

Figure 3. Sample residual gloss after irradiation with UVB light.

Considering the GSB Quality Standard AL 631 [24], which classifies a coating as extremely durable if it maintains at least 50% of the initial gloss after 1000 h UVB irradiation, it is possible to state that all the samples also showed a very good behaviour after 1000 h UVB exposure and met the industrial qualitative standards. The decrease of gloss is closely linked to the increase in roughness, as shown in Table 3.

3.3. Color Evaluation after UV Exposure

Ultraviolet radiation exposure could influence the aesthetic properties of the coatings, changing the colour or aspect of the coating surface. Figure 4a shows the as-prepared samples, and Figure 4b reports their colorimetric coordinates (CIE$L^*a^*b^*$ [25]) in order to appreciate the colour differences among the samples. The colorimetric coordinates values are the average of five measurements at D65/10° in SCE mode; L^* is the lightness (0 is black and 100 is white), a^* is the red-green coordinate (positive values are red, negative values are green), and b^* is the yellow-blue coordinate (positive values are yellow, negative values are blue, and 0 is neutral).

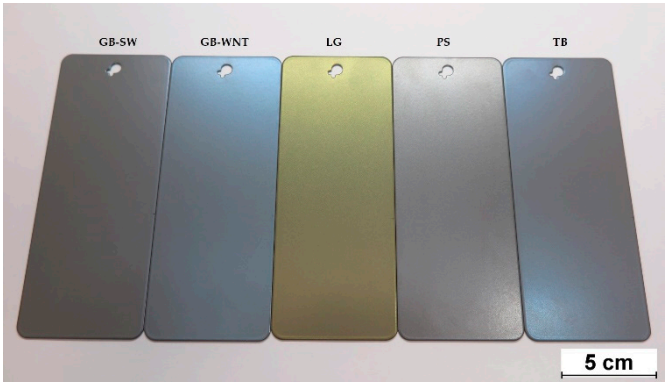

(**a**)

Sample	L*	a*	b*
GB-SW	52,94 ± 0,05	-0,46 ± 0,01	-0,68 ± 0,10
GB-WNT	53,28 ± 0,02	-0,74 ± 0,02	-1,65 ± 0,09
LG	52,63 ± 0,08	0,27 ± 0,02	9,45 ± 0,16
PS	50,30 ± 0,09	0,13 ± 0,03	-0,17 ± 0,07
TB	53,22 ± 0,14	-0,61 ± 0,01	-1,36 ± 0,10

(**b**)

Figure 4. (**a**) Photography of the as-prepared samples; (**b**) Samples' colorimetric coordinates according to CIE$L^*a^*b^*$.

All the samples showed a high lightness. Regarding the a^* value, it is possible to see that only the PS and LG samples had positive values, whereas, considering the b^* coordinate, all the samples showed a negative value, apart from the LG sample, which had a high shift towards yellow.

The colour of the coating was evaluated at the same cycles respect to the gloss and roughness measurements. The variation of ΔE, ΔL*, Δa*, Δb* are reported as a function of the exposure time. The symbol ΔE represents the total colour change and it is calculated as follows:

$$\Delta E = [(\Delta L^*)^2 + (\Delta a^*)^2 + (\Delta b^*)^2]^{1/2}, \quad (1)$$

(ASTM E308(2018) [26]). First of all, it is necessary to point out that no significant changes of ΔE, ΔL^*, Δa^*, Δb^* after UVA exposure were recorded. The ΔE variation was lower than 0.40 after 1000 h irradiation, and it did not increase with the exposure time. The variation of the a^* coordinate was negligible, whereas the variation of the b^* coordinate followed a blue shift trend for all the samples and in particular for the PS sample, which had a Δb^* equal to 0.60. Thus, it is possible to state that after irradiation with UVA light the ΔE variation was mainly due to the change of the b^* coordinate and was limited to low values (colour changes with $\Delta E < 1$ are imperceptible to the human eye).

Figure 5 reports the variation of the sample colorimetric coordinates after irradiation with UVB light.

The ΔE variation followed a sigmoidal trend for all the samples, with values after 1000 h irradiation included between 1.4 and 1.9, much higher than the threshold value of $\Delta E = 1$. Despite all the coatings being made of the same polymetric matrix, it was possible to observe the GB-NWT and PS samples having a ΔE change that was smaller with respect to the other three samples. These two pigments have a similar chemical composition, as they both contain Zr. Zirconium oxide is used in a huge variety of applications, such as in optical layers and pigments [27], because of its superior chemical and optical properties. It has a high index of refraction, optimal, chemical, and thermal stability, in addition to the fact that it has been demonstrated as increasing the photostability of the TiO_2 layer [28,29]. The presence of ZrO_2 could increase the photostability of the pigments, thus limiting their degradation and aesthetical property changes. The variation of ΔE is mainly due to a variation of brightness, L^*, which follows a sigmoidal trend as well. Making a comparison with the colour variation and the gloss trend, shown in Figure 3, it is possible to observe that the degradation process started after 300 h of UVB irradiation. The a^* parameter was included between 0.1 and −0.35; the LG and GB-SW pigments showed quite a negative variation. Regarding the b^* parameter, it varied from 0.10 to −0.50; the only sample which showed a positive increment of b^* was the GB-SW sample, whereas the LG pigment showed a major change of the b^* coordinate.

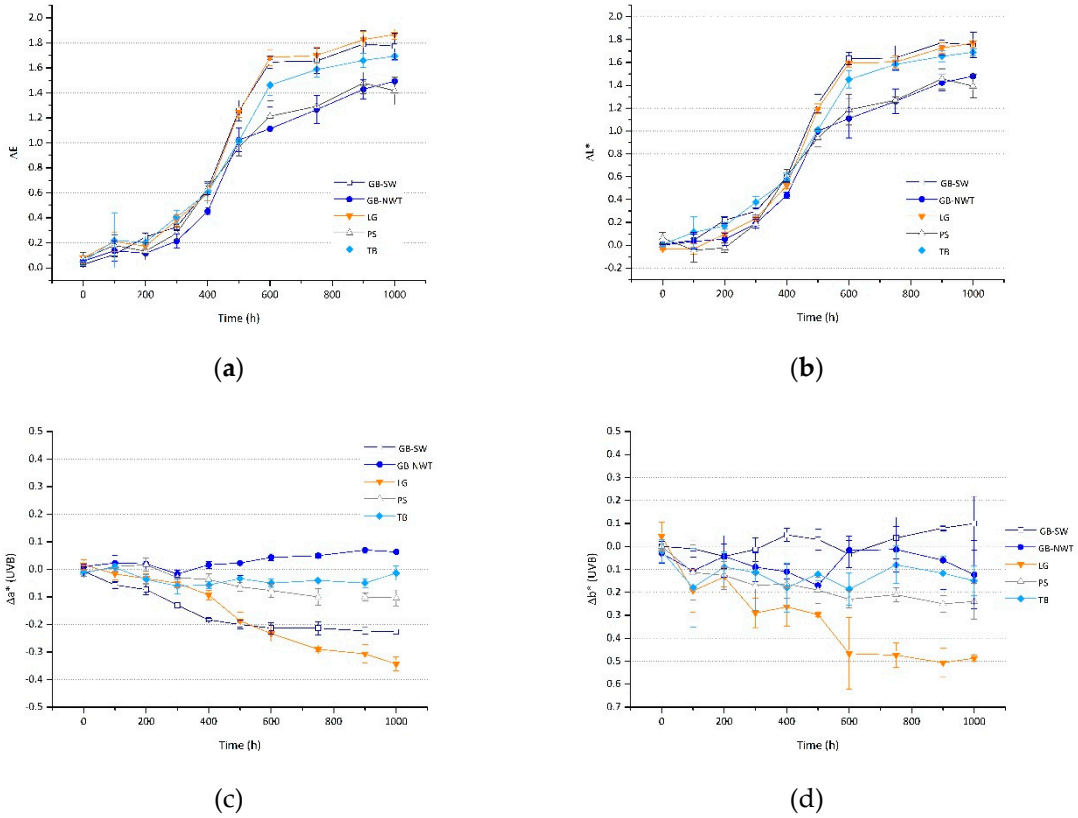

Figure 5. Colorimetric coordinates variation after UVB light exposure: (**a**) Δ*E*; (**b**) Δ*L**; (**c**) Δ*a**; and (**d**) Δ*b**.

3.4. FT-IR Analysis after UVA and UVB Exposures

In order to investigate the degradation and durability of powder coatings, FT-IR analyses were performed. Powder coatings based on polyesters, and in particular based on IPA, are used to withstand weathering, and they show an increased weathering resistance with respect to other coatings [30,31]. Different degradation mechanisms can affect the durability of superdurable resins [32], though the photo-induced oxidation mechanism is the most powerful and is mainly caused by resin absorbing UV radiation. The wavelengths between 290 and 370 nm cause important damages to the coatings because they lead to a change in the chemical structure of the polymeric matrix. Figure 6 shows the FT-IR spectra of the GB-SW sample before and after 1000 h of UVA exposure. It is possible, as a first thing, to assign the main peaks of the spectra.

A strong characteristic band associated with the carbonyl C=O stretching could be identified at 1715 cm^{-1} [31]. The peak at 1652 cm^{-1} can be associated to the C=O stretching of the curing agent typically used in this type of coatings [32]. The peak at 1608 cm^{-1} is related to the –CH– isophthalic bond stretching of the aromatic ring present in the isophthalic acid. The peaks at 1300 cm^{-1} and 1220 cm^{-1} are typical of C–O stretching. The peak at 1473 cm^{-1} could be both the bending of the $–CH_2–$ aliphatic group and the C=O bending; the peak at 1373 cm^{-1} corresponds to the CH_3 bending. The peak at 1072 cm^{-1} is related to the bending of aromatic C–H. No differences between the sample before and after UVA exposure could be detected. The same behaviour was followed by all the other samples, thus indicating that UVA radiation did not have an appreciable effect on the powder coating degradation.

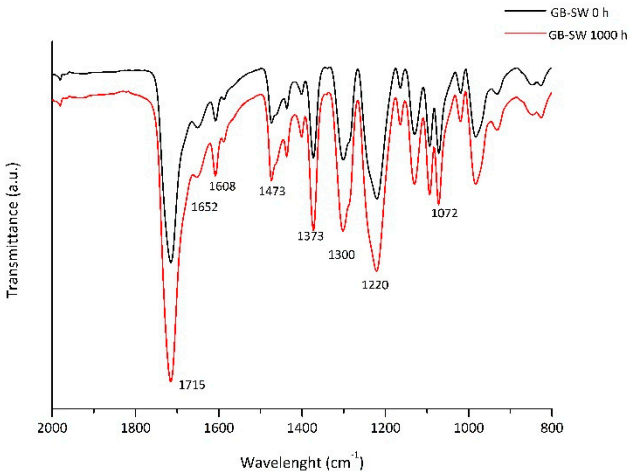

Figure 6. FT-IR spectra of the GB-SW sample before and after 1000 h of UVA exposure.

Instead, regarding the results obtained for the samples after UVB exposure, some differences could be noticed. Figure 7 shows the FT-IR spectra before and after 1000 h of UVB exposure.

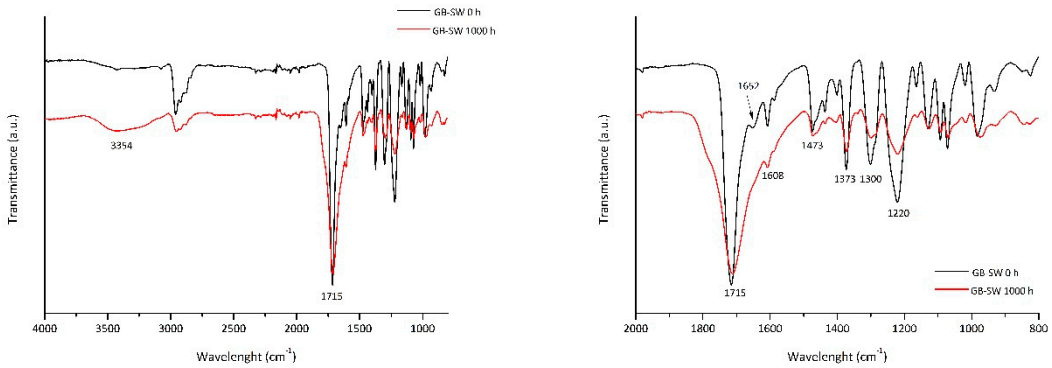

(**a**) (**b**)

Figure 7. FT-IR spectra of the GB-SW sample before and after 1000 h of UVB exposure: (**a**) reference spectra; (**b**) close-up of the (**a**) image.

Most of the peaks are shifted to lower wave numbers and have a lower transmittance, mainly due to the increase in mobility of the bonds with the absorption of UVB radiation. The two typical peaks of polyester at 1715 and 1652 cm^{-1} were different after 1000 h of exposure. The first peak underwent a shift towards 1711 cm^{-1} and a considerable broadening, whereas the latter almost disappeared. After UVB irradiation, a large band at 3354 cm^{-1} appeared, which could be associated with the –OH stretching vibration of hydroxyl groups, which may originate in the terminal phase of the degradation mechanism, already explained by Maetens [32]. The same behaviour was followed by all the five-sample series. It is then interesting to evaluate the FT-IR spectra of the samples at short exposure times, as shown in Figure 8.

The peak at 3354 cm^{-1} appeared after 300 h irradiation, while at the same time the peak at 1652 cm^{-1} disappeared. This change is the evidence of the initiation of the degradation process. All the samples followed the same trend shown for the GB-SW sample. A photo-induced oxidation mechanism generated by a photo-inductor can explain these results [32]. The samples exposed to UVB light underwent a degradation process starting from 300 h of irradiation, which can be correlated to the sample colour change shown in Figure 5.

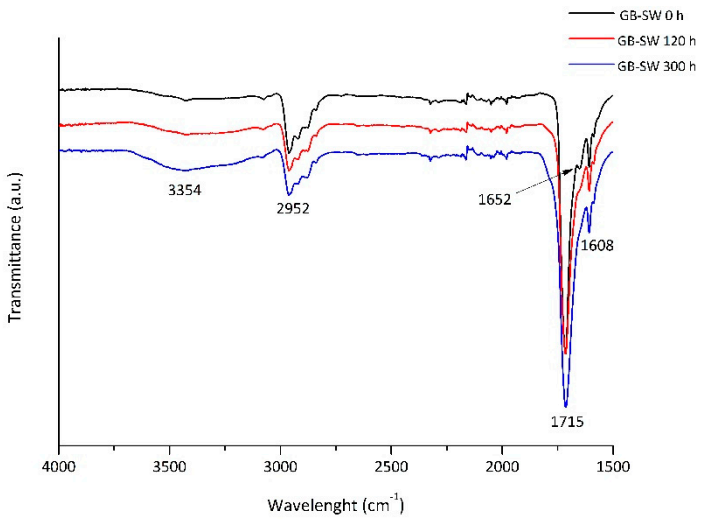

Figure 8. FT-IR spectra of the GB-SW sample before exposure, after 120 h, and after 300 h of UVB irradiation.

3.5. Exposure to an Aggressive Environment: Acetic Salt Spray Exposure

In order to determine the protective properties of the coatings and assess the adhesion of the coating with respect to the substrate, the samples were exposed to acetic salt spray fog for 1000 h in the presence of an artificial defect. As it is possible to observe in Figure 9, all the samples showed the presence of blisters of grade 4 (S5) [33], limited to the borders and the area close to the artificial defect. In addition to that, all the samples showed no blistering until 650 h of exposure, underlining the good protection properties of the coatings. In any case, it is important to point out that the evaluation of the blistering grade should be done on as-made samples, without the presence of an artificial scratch: considering the area far from the defect, no blisters could be observed.

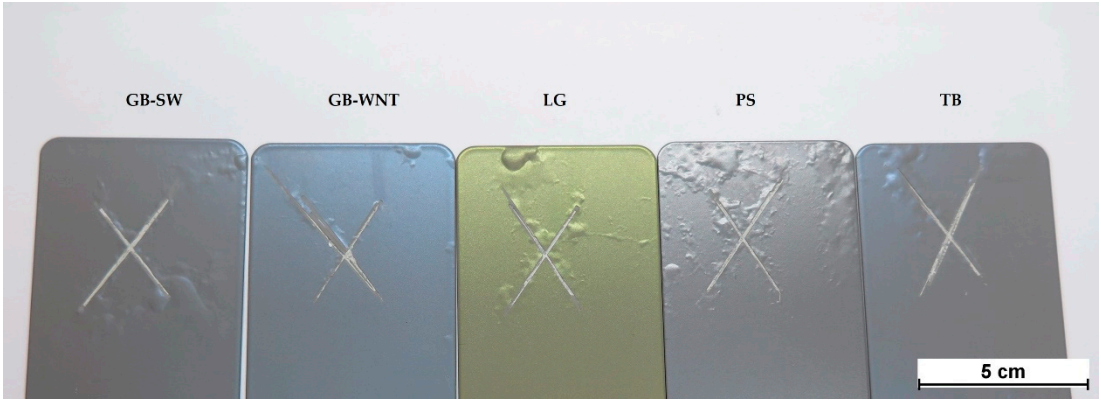

Figure 9. Samples after 1000 h exposure in an acetic salt spray chamber in the presence of an artificial scratch.

A delamination and corrosion assessment was carried out on the sample in presence of the artificial scratch, according to the UNI EN ISO 4628-8 standard [20]: the values obtained for delamination were included between 4.0 and 8.0 mm, the values obtained for corrosion were about 5 mm for all the samples.

Only small differences among the different samples could be observed. The slightly different thicknesses of the coatings does not represent an influencing factor since in this case the mechanism that could lead to a loss of adhesion between the coating and the substrate was represented by anodic undermining (typical of painted aluminium alloys), which is not influenced by the coating thickness,

unlike what occurs in cathodic delamination [34]. The substrate pre-treatment could influence the adhesion of the coating on the substrate [35], then leading to the formation of blisters, but it is difficult to add this motivation to explain little differences between samples. On the contrary, these differences could be explained by little fluctuations of temperature or humidity in the deposition processes, which can have a negative influence on the adhesion with the substrate. It is necessary to underline that no relevant studies regarding the effect of aluminium-based pearlescent pigments on the degradation of powder coatings can be found in the literature, but it is reasonable to state that the different pigments have no influence on the degradation of the samples.

In order to have further insights on the protection properties of the coatings, EIS measurements were carried out before and after 400 h, 750 h, and 1000 h of exposure in an acetic salt spray chamber on as-made samples. In Figure 10, the Bode diagram of the GB-SW sample is shown. It is possible to observe that the impedance modulus |Z| at 10^{-2} Hz remained stable in time with a value of around 10^{11} Ω·cm^2, typical of protective organic coatings. Thus, the coating can be considered highly protective also after exposure to an aggressive environment.

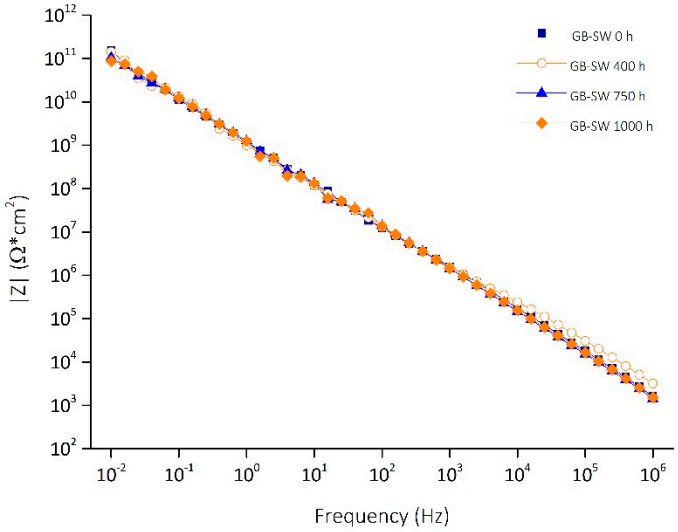

Figure 10. Bode diagram of the GB-SW sample at different acetic salt spray exposure times.

All the samples show a similar behaviour, and the impedance modulus |Z| versus applied frequency follows the same trend. Table 4 reports the values of |Z| at 10^{-2} Hz after 0, 400, 750, and 1000 h of acetic salt spray exposure for all the samples under investigation.

Table 4. Impedance modulus |Z| (Ω*cm^2) at 10^{-2} Hz after 0, 400 h, 750 h, and 1000 h.

Coating Name	0 h	400 h	750 h	1000 h
GB-SW	1.56×10^{11}	1.43×10^{11}	1.06×10^{11}	8.66×10^{10}
GB-WNT	1.57×10^{11}	1.06×10^{11}	8.66×10^{10}	8.40×10^{10}
LG	1.66×10^{11}	1.38×10^{11}	9.25×10^{10}	8.67×10^{10}
PS	1.23×10^{11}	8.67×10^{10}	6.70×10^{10}	6.23×10^{10}
TB	1.59×10^{11}	1.38×10^{11}	9.58×10^{10}	8.69×10^{10}

All the samples, as shown in Table 4, maintain a very high value of the impedance modulus, also after 1000 h of acetic salt spray exposure. Thus, it is possible to confirm that all the samples, without the presence of surface defects, can guarantee optimal protection properties, regardless of the used pigment.

4. Conclusions

This work examined the effect of five different pearlescent pigment types on standard powder coatings. The coatings' aesthetical and protective property changes were analysed as a consequence of accelerated ageing testing. The colour, gloss, and roughness were evaluated after UVA and UVB exposure. Regarding the samples subjected to UVA radiation, the surface colour did not register important changes, or, in any case, they were imperceptible to the human eye. Even the variation in gloss and roughness that was recorded was not significant. The results obtained after UVB exposure showed a different trend: the surface roughness showed a general increase, closely related to the decrease of gloss and the variation of colour. The decreasing gloss variation can be considered acceptable from a commercial point of view, while the colour change is very huge and could be attributable to the degradation of the polymeric matrix. The FT-IR analysis showed that UVB radiation caused a photoinduced degradation of the polymeric matrix, whereas the UVA radiation had no influence on the degradation of the coating. The degradation mechanism, due to UVB radiation, started after 300 h of exposure, and this is closely related to the abrupt change of colour and gloss. The analyses carried out after exposure to an acetic spray fog showed the good protection properties of the coating. EIS measurements showed that all the samples remained highly protective, also after 1000 h of acetic salt spray chamber exposure. In addition to that, all the samples showed no remarkable presence of blisters and detachment of the coating. On the other hand, a different behaviour in the presence of an artificial defect could be observed: a quite severe delamination and corrosion could be noticed. In conclusion, it is possible to state that these samples are very sensitive to UVB radiation but show good resistance to UVA light and to aggressive environments without the presence of coating defects. No pigment effect on the degradation of the samples could be revealed, though some differences in colour changes could be seen among the different sample types, which can be attributed to changes in the chemical composition.

Author Contributions: Project Administration, S.R.; Supervision, S.R.; Investigation, L.B.R.; Formal Analysis, L.B.R., F.R.; Data Curation, F.R.; Writing–Original Draft Preparation, F.R.; Writing–Review, S.R. All authors have read and agreed to the published version of the manuscript.

Funding: This research received no external funding.

Acknowledgments: The authors gratefully acknowledge Akzo Nobel Coatings S.p.A. (Como, Italy) in the person of Roberto Paganica and Merck Italia S.p.A. (Milano, Italy) in the person of Stefano Corrado for supplying the coated samples and the pigments, respectively.

Conflicts of Interest: The authors declare no conflict of interest.

References

1. Ashby, M.F.; Johnson, K. *Materials and Design: The Art and Science of Material Selection in Product Design*, 2nd ed.; Butterworth-Heinemann: Oxford, UK, 2009.
2. Rossi, S.; Deflorian, F.; Scrinzi, E. Reduction of aesthetical properties of organic coatings caused by mechanical damage. *Mater. Des.* **2009**, *30*, 1511–1517. [CrossRef]
3. Perera, D.Y. Effect of pigmentation on organic coating characteristics. *Prog. Org. Coat.* **2004**, *50*, 247–262. [CrossRef]
4. Pfaff, G.; Franz, K.; Emmert, K.; Nitta, R. Pigments, Inorganic. In *Ullmann's Encyclopedia of Industrial Chemistry*, 6th ed.; Wiley-VCH: Weinheim, Germany, 1998.
5. Bauxbaum, G.; Pfaff, G. *Industrial Inorganic Pigments*, 3rd ed.; Wiley-VCH: Weinheim, Germany, 2005. [CrossRef]
6. Jansen, M.; Letschert, H.P. Inorganic yellow-red pigments without toxic metals. *Nature* **2000**, *404*, 980–982. [CrossRef] [PubMed]
7. Wendusu, T.; Masui, T.; Imanaka, N. Novel environmental-friendly inorganic red pigments based on (Bi, Er, Y, Fe)$_2$O$_3$ solid solutions. *J. Asian Ceram. Soc.* **2014**, *2*, 195–198. [CrossRef]
8. Faulkner, E.B.; Schwartz, R.J. *High Performance Pigments*, 2nd ed.; Wiley-VCH: Weinheim, Germany, 2009. [CrossRef]

9. Maisch, R.; Weigand, M. *Pearl Luster Pigments, Physical Principles, Properties, Applications*; Verlag Moderne Industrie: Landsberg, Germany, 1992.
10. Pfaff, G. *Special Effect Pigments: Technical Basics and Applications*; Vincentz Network GmbH & Co KG: Hannover, Germany, 2008.
11. Maile, F.J.; Pfaff, G.; Reynders, P. Effect pigments – past, present and future. *Prog. Org. Coat.* **2005**, *54*, 150–163. [CrossRef]
12. Maisch, R.; Stahlecker, O.; Kieser, M. Mica pigments in solvent free coatings systems. *Prog. Org. Coat.* **1996**, *27*, 145–152. [CrossRef]
13. Pfaff, G.; Becker, M. Special effect pigments in cosmetic applications. *Househ. Pers. Care Today* **2012**, *1*, 12–15.
14. Pfaff, G. Special effect pigments based on silica flakes. *Inorg. Mater.* **2003**, *39*, 123–126. [CrossRef]
15. *ASTM G154-16 Standard Standard Practice for Operating Fluorescent Ultraviolet (UV) Lamp Apparatus for Exposure Non-Metallic Materials*; ASTM International: West Conshohocken, PA, USA, 2016.
16. *ASTM D523-14(2018) Standard Standard Test Method for Specular Gloss*; ASTM International: West Conshohocken, PA, USA, 2018.
17. *ISO 4288:1996 Standard Geometrical Product Specification (GPS)—Surface Texture: Profile Method—Rules and Procedures for the Assessment of Surface Texture*; International Organization for Standardization: Geneva, Switzerland, 2018.
18. *ASTM B117-19 Standard Standard Practice for Operating Salt Spray (Fog) Apparatus*; ASTM International: West Conshohocken, PA, USA, 2019.
19. *ASTM G85-19 Standard Standard Practice for Modified Salt Spray (Fog) Testing*; ASTM International: West Conshohocken, PA, USA, 2019.
20. *UNI EN ISO 4628-8(2013) Standard Evaluation of Degradation of Coatings—Designation of Quantity and Size of Defects, and Intensity of Uniform Changes in Appearance—Part 8*; UNI Ente Nazionale Italiano di Unificazione: Milano, Italy, 2013.
21. Topuz, B.B.; Gündüz, G.; Mavis, B.; Çolak, Ü. The effect of tin dioxide (SnO_2) on the anatase-rutile phase transformation of titania (TiO_2) in mica-titania pigments and their use in paint. *Dye. Pigm.* **2011**, *90*, 123–128. [CrossRef]
22. Gao, Q.; Wu, X.; Fan, Y. The effect of iron ions on the anatase-rutile phase transformation of titania (TiO_2) in mica and titania pigments. *Dye. Pigm.* **2012**, *95*, 96–101. [CrossRef]
23. Hosseini Zori, M. Particle size and kind of mica in synthesis of nontoxic bronze and gold pearlescent pigments based on nanoencapsulated hematite. *J. Ultrafine Grained Nanostruct.* **2015**, *48*, 101–112. [CrossRef]
24. *GSB AL 631 Standard, "International Quality Regulations for the Coating of Building Components—Aluminium"*; GSB International e.V.: Düsseldorf, Germany, 2017.
25. Hunter, R.S.; Harold, R.W. *The Measurement of Appearance*, 2nd ed.; John Wiley & Sons: Hoboken, NJ, USA, 1987.
26. *ASTM E308-18 Standard, "Standard Practice for Computing the Colors of Objectives by Using the CIE System"*; ASTM International: West Conshohocken, PA, USA, 2018.
27. Zhang, Q.; Shen, J.; Wang, J.; Wu, G.; Chen, L. Sol-gel derived ZrO_2–SiO_2 highly reflective coatings. *Int. J. Inorg. Mater.* **2000**, *2*, 319–323. [CrossRef]
28. Wei, B.-X.; Zhao, L.; Wang, T.-J.; Gao, H.; Wu, H.-X.; Jin, Y. Photo-stability of TiO2 particles coated with several transition metal oxides and its measurements by rhodamine-B degradation. *Adv. Powder Technol.* **2013**, *24*, 708–713. [CrossRef]
29. Mathivanan, L.; Arof, A.K. The effect of zirconium oxide and quartz pigments on the heat and corrosion resistance properties of the silicone based coatings. *Pigm. Resin Technol.* **2000**, *29*, 10–15. [CrossRef]
30. Rossi, S.; Fedel, M.; Petrolli, S.; Deflorian, F. Behaviour of different removers on permanent anti-graffiti organic coatings. *J. Build. Eng.* **2016**, *5*, 104–113. [CrossRef]
31. Gheno, G.; Ganzerla, R.; Bortoluzzi, M.; Paganica, R. Accelerated weathering degradation behaviour of polyester thermosetting powder coatings. *Prog. Org. Coat.* **2016**, *101*, 90–99. [CrossRef]
32. Maetens, D. Weathering degradation mechanism in polyester powder coatings. *Prog. Org. Coat.* **2007**, *58*, 172–179. [CrossRef]
33. *UNI EN ISO 4628-2(2016) Standard, "Evaluation of Degradation of Coatings—Designation of Quantity and Size of Defects, and Intensity of Uniform Changes in Appearance—Part 2"*; UNI Ente Nazionale Italiano di Unificazione: Milano, Italy, 2016.

34. Mirabedini, S.; Scantlebury, J.D.; Thompson, G.E.; Moradian, S. Adhesive strength of powder coated aluminium substrates. *Int. J. Adhes. Adhes.* **2005**, *25*, 484–494. [CrossRef]
35. Fedrizzi, L.; Stenico, M.; Deflorian, F.; Maschio, S.; Bonora, P.L. Effect of powder painting procedures on the filiform corrosion of aluminium profiles. *Prog. Org. Coat.* **2007**, *59*, 230–238. [CrossRef]